Chapter 5

Dimensionality analysis of the study area

According to the regional geologic features of the Central Andes, an approximately N-S magnetotelluric regional strike is expected, if the MT data are to reliably represent a 2-D conductivity model. The first step is to analyze the dimensionality of the data and to investigate whether a 2-D model for the region (or partly) can be assumed (section 5.1).
The regional strike angles are determined by two different tensor decomposition schemes (section 5.2). Both are based on the superposition model hypothesis (i.e., shallow 3-D anomalies overly a regional 2-D structure; (section 1.2)), where galvanic distortions affect the measured data. Section 1.2.5 presents the application of the telluric decomposition (Groom & Bailey, 1989; section 5.2.2) and section 5.2.1 the telluric and magnetic decomposition (Chave, 1994; section 1.2.6).
The single site regional strikes obtained from the telluric decomposition ranged indeed near N-S, with the exception of the Precodillera and the eastern Altiplano regions where the test of the hypothesis (χ^2 misfit) indicated the non validity of the regional 2-D model.
The strike angles after the telluric and magnetic tensor decomposition pointed to -8°N between the Coastal Cordillera and western Precordillera for short period data (<1000 s), whereas no consistent angles were obtained either to the east or at longer period data.
The decomposition schemes also allow a quantification of the telluric distortion, observed in the twist and shear angles. Maximal shear values −indicative of strong galvanic distortions− were obtained at several sites from the Coastal Cordillera and Precordillera. The strike differences between both decomposition methods as well as the non validity of the 2-D regional model in the Precordillera are due to this strong distortion, which was investigated and explained in detail by a current channeling analysis (chapter 6.1). Thereby the anomalies -cause of the distortion- are identified qualitatively in the different regions (section 6.3).

5.1 The phase sensitive skew parameter

Based on the hypothesis that telluric distortion affects the impedance tensor, produced by shallow 3-D anomalies overlying a regional 2-D structure (2-D superposition model; section 1.2.3), the phase sensitive skew parameter defined by Bahr [1988] (section 1.2.4) was calculated for each site as a function of periods.
This non-dimensional parameter can be interpreted as a measure of galvanic distortion, whenever the superposition model is valid. A zero skew value indicates the validity of the 2-D superposition model, if galvanic magnetic effects are negligible and data are noise free. Values over 0.3 can be considered as an indicator of true 3-D inductive regional structures (Bahr [1988]).

Since the rotational invariant skew parameter is a non-linear function of the impedance tensor elements, it can be subject to strong bias by noisy data and therefore a confidence limit of skew, based on a conditional probability function dependent of the diagonal tensor elements (Section 2), will be regarded instead of the value itself. In our data the skew bias

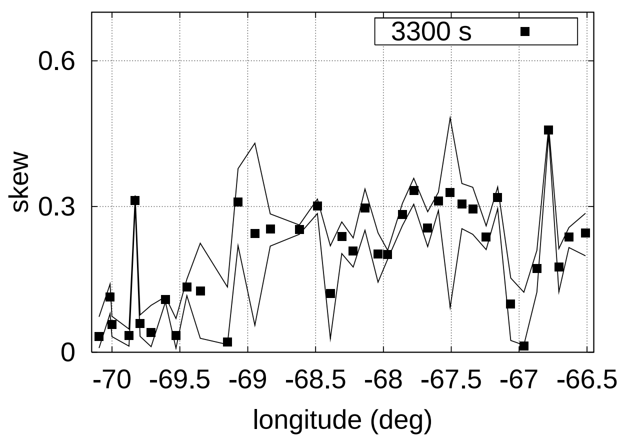

Figure 5.1: Measured skew values (dots) within the 95% confidence limit (lines) of the Ancorp profile. Data correspond to the period 3300 s.

is usually observed at either the shortest periods or at longer periods (>1000 s), where the diagonal tensor element Re, ImZ_{xx} treated as the random variable (section 2) gives a broader confidence limit than by treating the element Re, ImZ_{yy}.
An example of the skew bias is shown for the Ancorp profile for data within the 95% confidence limit at the period of 3000 s (fig.5.1). We will regard hereafter all skew values as the upper boundary of the confidence limit. Thus the shown skew is the value in which the real skew has the 97.5% probability to lay below this. Since the impedance errors are very small in the period range $100-1000$ s, the measured skew coincides with the 95% probability, i.e., skew is not biased.

In order to have an overview of the whole measured area, the 97.5% probability thresholds of the skew parameter are interpolated between the sites and illustrated in W-E pseudo sections as a function of period (fig.5.2). The plots show the values of the Pica and Ancorp traverses (see fig.4.1) and a third W-E projection of the sites in between.
At short (> 20 s) and long periods (fig.5.2) we can observe small skew values (<0.3) in the Coastal Cordillera (CC; 70 to 69.5°W). In the region between the Long Valley (LV) and the

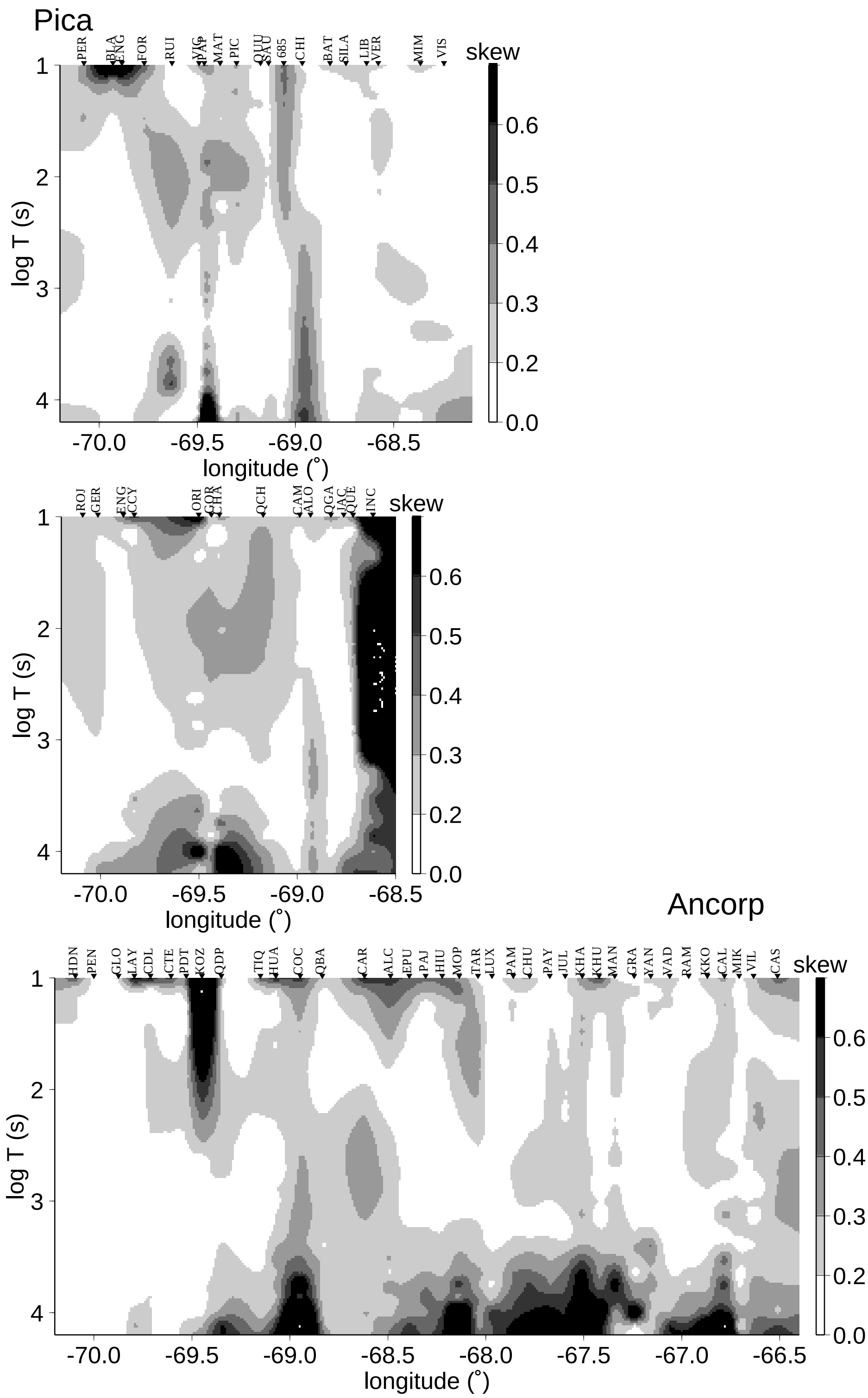

Figure 5.2: Interpolated skew values (Bahr [1988]) as a function of the logarithmic period for the Pica(*above*) and Ancorp(*below*) profile (fig.4.1) projected in W-E traverses. The centre plot is the projection of the sites in between. The skew values are the 97.5% probability thresholds. Small skews (f. ex., < 0.3) can indicate the validity of a regional 2-D conductivity structure.

Precordillera (PC; 69.5 to 68.5°W), the values are in average higher than to the east and west. Therefore we observe that the probability that the data at the mid period band in LV and PC is affected by 3-D inductive effects is high (i.e., skew > 0.3), whereas in CC and the Altiplano (AP) the 2-D superposition model hypothesis is supported with higher confidence. In the middle profile, site INC located in WC (-68.5) has extremely high values for periods > 500 s (dark colors; fig.5.2).
In the Ancorp profile, data in the W. Cordillera and Altiplano reach extreme values at longer periods (>3000 s), as well as site COC located in between the Precordillera fault system. Also, along this fault (at 69°W), the data of sites ALO and CHI (mid- and Pica profile) surpass 0.3 at long periods.

The previous analysis leads to the conclusion that the Coastal Cordillera data support a 2-D superposition model at almost all periods (f.ex., sites ENG and ROJ in fig.5.3), where galvanic distortions produced by local anomalies affect the impedances.
In the Longitudinal Valley the 2-D superposition model hypothesis can be considered valid at longer periods (600−3000 s, site GOR and PDT in fig.5.3).
In the Precordillera, data from site to site show different behaviours with the period (site 685 and QBA in fig.5.3). While data from sites located along the Precordillera fault system (at 69°W; CHI, ALO and COC) show a common feature, a low probability for the validity of the superposition model at long periods, some sites to the east and west of this longitude show in contrast a less probable superposition model assumption at short and/or mid-period range.
The heterogeneous skew behaviour seen in the Precordillera leads us to infer that a complex conductivity structure beneath the Precordillera fault system can explain the measured data. This observation is also in agreement with the 3-D behaviour of the induction arrows (fig.4.3) as well as the MT phases of the N-S electric field component running out of the I quadrant (>90°; fig.4.2; left)).
In the Western Cordillera one can optimistically assume the validity of the superposition model (site VER in fig.5.3), although the skew values in the Ancorp profile are just beyond the limits (0.3) for the shortest and longest period data (site MOP in fig.5.3).
In the Altiplano the superposition model is mostly supported by the mid period band data (<3000 s; site Jul in fig.5.3). Instead, large skew values reflect a regional 3-D conductivity structure and/or bad data quality at longer periods (right plots of fig.5.3).

If the 2-D superposition model is valid, a consistent regional strike should be found for the region under study.

5.2 Determination of regional 2-D strike

In this section are shown two different decomposition schemes to investigate the regional 2-D strike and the amount of telluric distortion affecting the data.
The telluric tensor decomposition method (Groom and Bailey [1989b]) was applied to the MT data and an approximately N-S regional strike was found (section 5.2.1), though the χ^2 test

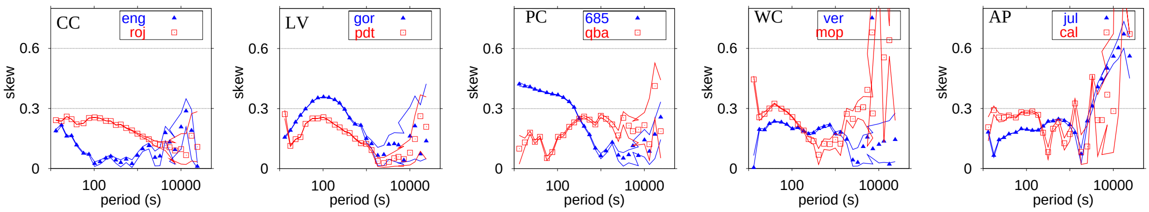

Figure 5.3: Skew values as function of period for several sites distributed along the study area. The measured skew (triangles and squares) is shown within the 95% confidence limit (lines). The plots show each two sites for the same geological unit (North in red, south in blue). The graphic distribution is according from west to east: CC=Coastal Cordillera, LV=Longitudinal Valley, PC=Precordillera, WC=Western Cordillera, AP=Altiplano.

of the hypothesis indicates non-validity of the model in the Precordillera and the Altiplano data.
Since induction arrows showed evidence that lateral conductivity contrasts are not necessarily N-S oriented −thus magnetic effects are present− the telluric and magnetic tensor decomposition scheme (Chave and Smith [1994]) was applied to the MT and magnetic transfer function data (section 5.2.2). A regional strike of -8°N at short period data (<1000 s) was found from the coast to the Precordillera, in accordance with the hypothetical event analysis formulated by Ritter [1996], applied for the magnetic transfer functions of the Pica profile (Echternacht [1998]).

5.2.1 Telluric tensor decomposition

The Groom & Bailey (1989) tensor decomposition is applied to the measured data in order to find the single site regional strike angles. The method is based on the telluric distortion assumption produced by small shallow 3-D anomalies (section 1.2.5). The hypothesis is tested with the χ^2-misfit function (section 1.2.5), which is a measure for the validity of the superposition model.
The decomposition was calculated for each site by varying the strike angle by steps of 5° between -45° and 45° (0° denotes the measured coordinate system), calculating the χ^2 misfit between measured and decomposed impedances for each fixed angle. Then at each site, the regional strike corresponds to the minimum averaged χ^2 misfit calculated for the period band. This procedure was performed separately for a short (50-1000 s) and a long period band (1000-6000 s). Since near surface induction effects decrease with depth it is to be expected that longer period data should be more suitable for the telluric distortion model.
The single site strike angles obtained for the two period bands are shown in fig.5.4.

In the Coastal Cordillera (CC: -70 to -69.5°) are found the most stable strike angles. In both period bands the variation of the values remains near 0°. Also, the χ^2 misfit is small, which is in accordance with the small skew values supporting the telluric model (section 5.2).
For the long perionad band the single srike angles from CC to PC regions (-70 to -69°) are more stable around 0°. The exceptions are sites ORI and CHI located in the Longitudinal Valley

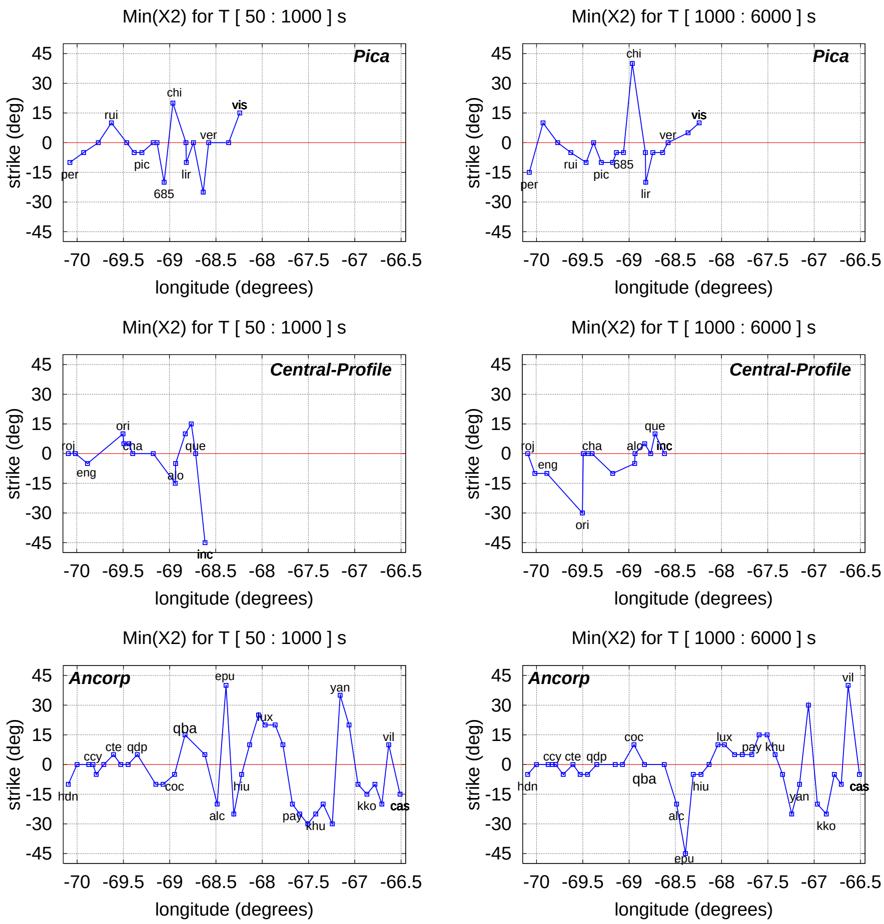

Figure 5.4: Regional magnetotelluric strike directions for the sites along the Ancorp profile (bottom), Pica profile (top) and the sites in between (center). The solution was obtained by the telluric tensor decomposition (Groom and Bailey [1989b]) for fixed strike angles of the minimal period averaged χ^2 misfit. *Left:* Procedure performed in the period range 50-1000 s. *Right:* Procedure performed in the period range 1000-6000 s.

(LV) and PC, respectively (central profile in fig.5.4). In the Ancorp profile, near 0° strike angles are also seen in between the Western Cordillera (WC) and western Altiplano (AP). The minimum period averaged χ^2 misfit for the sites having strike angles near 0° are considerably smaller in CC and LV than those from the adjacent regions. Thus the superposition model is more reliable in the Coastal Cordillera.
An example of this procedure is illustrated in fig.5.5, where the χ^2 misfit for the whole period band is shown. An example of the near 0° consistent strike angle found in CC for the two selected period bands is shown for site ENG (Pica profile). In fig.5.4, site QBA (Ancorp profile) belongs to the unstable strike angles obtained for locations between PC and WC.
The twist and shear angles shown in fig.5.5 quantifies the degree of telluric distortion. Twist is the average electric field components rotation due to the distorter, and shear the angle difference between the two components. A maximal shear value (45°) indicates a strong galvanic distortion, where the electric fields are strongly polarized in one single direction (i.e., current channeling; section 6.1). Such a case is observed at sites located in the Coastal

Cordillera as well as in several sites from the Longitudinal Valley and Precordillera, as will be discussed later (section 6.3).

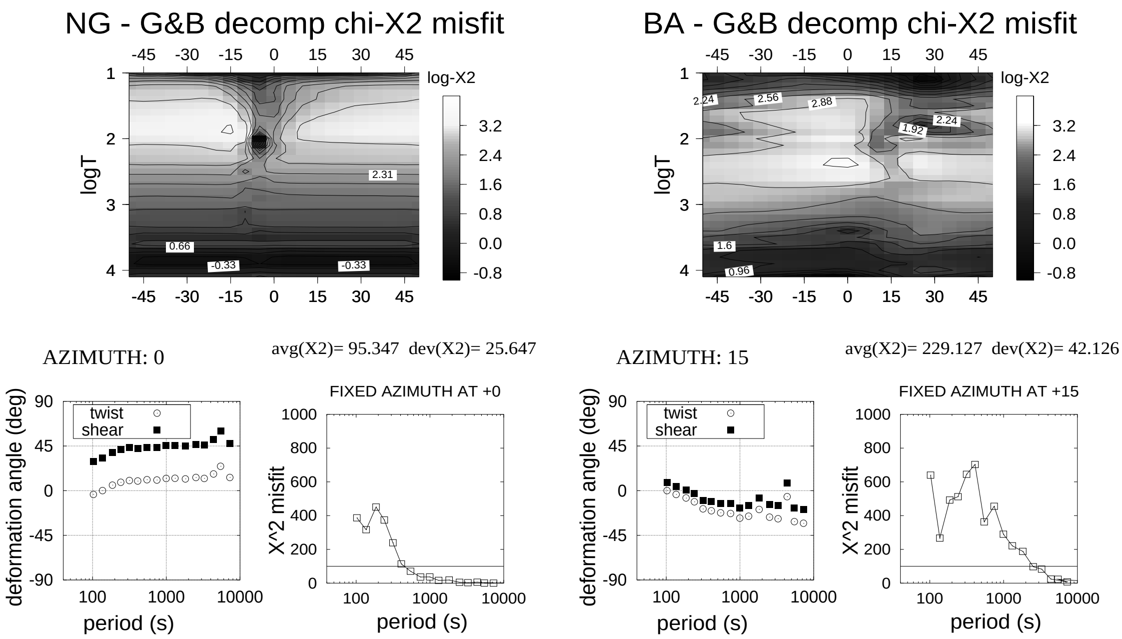

Figure 5.5: Example of the procedure followed in the single site regional strike determination of fig.5.4. Site ENG and QBA, located in the Coastal- (left) and Pre- Cordillera (right), respectively. The solution was obtained by the telluric tensor decomposition (Groom and Bailey [1989b]). The graphics *above* show the contour plots χ^2 misfit as a function of the fixed strike angles and logarithmic periods (log T). The graphics *below* show the twist and shear angles (left) and the χ^2 (right) as a function of period for the minimal period average χ^2 strike angle (fixed azimuth). dev(X2)= Standard deviation of the minimal period averaged χ^2 misfit (avg(X2)). Site QBA has far exceed an acceptable χ^2 test of the 2-D model hypothesis (avg(χ^2)¿100).

From the telluric decomposition analysis it was found that the regional strike is approximately N-S (or W-E if we consider the intrinsic $\pm 90°$ indeterminacy of the method) almost everywhere between the Coastal and Western Cordillera, where a regional 2-D model for the MT data to the east of CC becomes more reliable at higher penetration depths. Nevertheless, this does not mean that the 2-D superposition model hypothesis has been generally fulfilled, since the single sites' averaged χ^2 values have usually surpassed the expected values of a confident model fit in the Pre- and Western Cordillera site data (for ex., site QBA in fig.5.5). In the Altiplano no consistent strike angle is obtained.
It follows to analyze if the measured data can better support the superposition model by considering the magnetic effects.

5.2.2 Telluric and magnetic tensor decomposition

As in the telluric decomposition scheme, this method is based on the 2-D superposition model. Here magnetic effects are also considered (section 1.2.3). The Chave and Smith [1994] decomposition scheme is applied on the MT and GDS data, following the same procedure as described in section 5.2.1 for the single site regional strike determination. The step strike angles ranged between -90° and 90° in this case, since by the inclusion of the vertical magnetic field component in the decomposition the ±90° strike indeterminacy is avoided.

The obtained short and long period band strike angles are shown in fig.5.6. The angles vary with the site location, though less variation at the long period band is seen. The site angles tend to be similar to the site real induction arrow orientations at the corresponding period band. This clearly contradicts the previous telluric decomposition result. The exceptions are the Ancorp profile sites located between WC and western AP with strikes near 0°, which is in agreement with the approximate E-W real induction arrow directions.

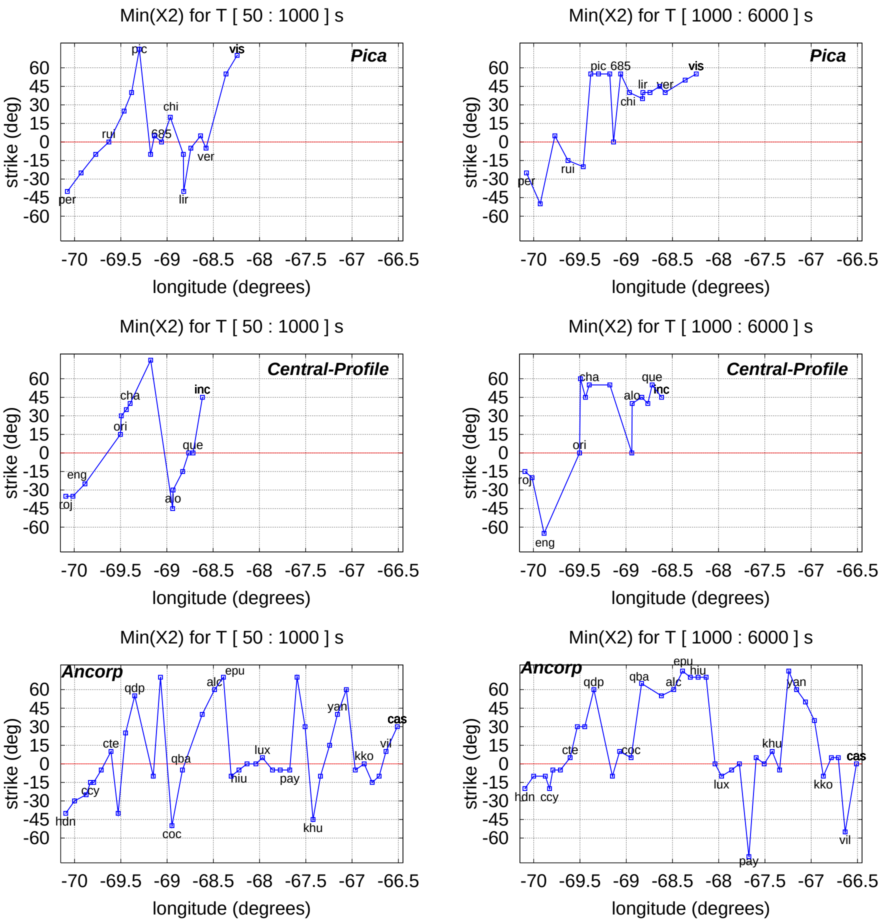

Figure 5.6: Regional strike directions for the sites along the Pica profile (above), Ancorp profile (bottom) and the sites in between (center). The solution was obtained by telluric and magnetic tensor decomposition (Chave and Smith [1994]) for fixed strike angles of the minimal period averaged χ^2 misfit. *Left:* Procedure performed in the period range 50-1000 s. *Right:* Procedure performed in the period range 1000-6000 s.

An example of the procedure is shown in fig.5.7 for the representative sites ENG (in CC) and QBA (in PC). For site ENG, the minimum averaged χ^2 value is seen clearly at the -20°N (c.c.w.) fixed azimuth[1], whereas the minimum χ^2 values at site QBA show strong

[1] In the Chave and Smith [1994] decomposition scheme, strike angles are defined positive c.w. with respect to the east. Thus, a 70° azimuth is equivalent to -20° with respect to North.

variation with period. The latter reflects the non-validity of the 2-D superposition model. The remarkable difference observed between ENG and QBA is analogous for the rest of the sites located in CC in comparison with those located in PC and WC. This effect leads to the observed strong strike angle variation among the sites at these locations. Also, the minimum χ^2 average value for a selected period band can fulfill different fixed strike angles. For example, observe in fig.5.7 that the χ^2 of site ENG for periods >1000 s are equally low at several different fixed strike angles.
In addition, for the selected fixed strike angles, shear is maximal at the sites located in the Coastal Cordillera, and at several sites in the Precordillera (fig.5.7). Thus strong galvanic distortion is again observed.

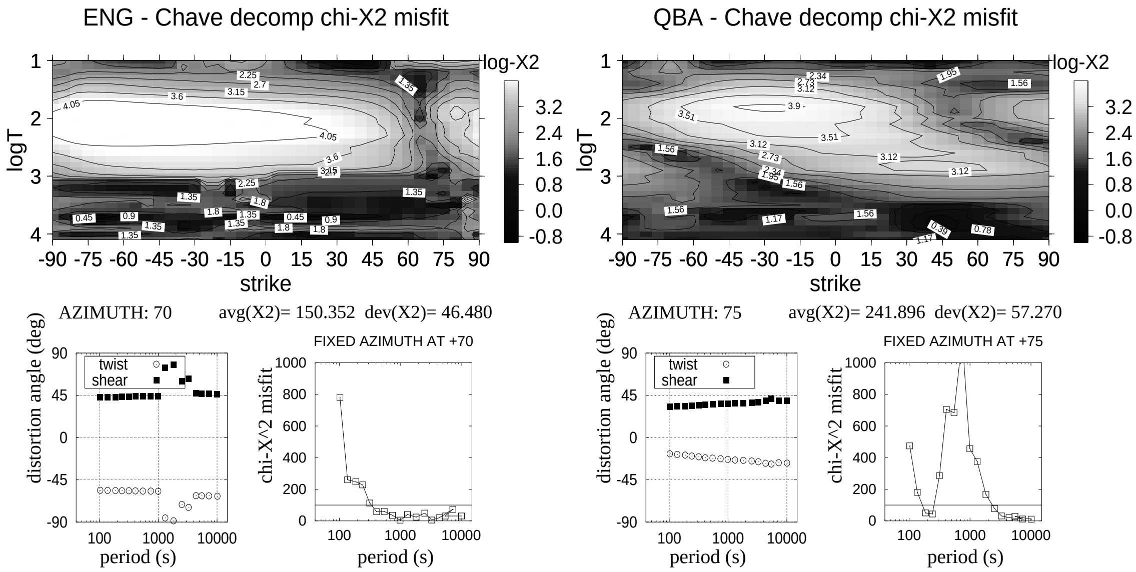

Figure 5.7: Example of the procedure followed in the single site regional strike determination of fig.5.6. Site ENG and QBA, located in the Coastal- (left) and Pre- Cordillera (right), respectively. The solution was obtained by the telluric and magnetic tensor decomposition (Chave and Smith [1994]). The graphics *above* show the contour plots χ^2 misfit as a function of the fixed strike angles and period. The graphics *below* show the twist and shear angles (left) and the χ^2 (right) as a function of period for the minimal period average χ^2 strike angle (azimuth; c.w. with respect to the east). In site QBA the large χ^2 values indicate the non-validity of the 2-D superposition model.

Since no consistent strike angle was found, the above results lead us to conclude that the 2-D superposition model under magnetic galvanic distortion is not valid in the region. Another factor could be the chosen procedure itself. Although the regional strike search by the minimum period averaged χ^2 reduces the number of model parameters (i.e., azimuth is defined as *a priori*), it seems that this is not enough to constrain the solution.
A method to constrain the solution and thereby constrain the regional strike between adjacent sites is to realize a multiple site decomposition. This means, the tensor decomposition is performed on the MT data of multiple sites and therefore a common solution is obtained (same strike angle and distortion parameters). The number of variables to solve (i.e., model parameters) is considerably reduced, since the solution gives frequency independent twist and shear parameters at each site, as well as a common fixed strike angle for the multiple sites.

Also, the degrees of freedom of the system will be increased the more sites are considered in the decomposition. This means, the expected χ^2 value of the hypothesis test is larger.
This multiple site decomposition is applied to the data. Several groups of sites are selected according to location and similar characteristics observed in the MT data. Choosing a certain group only under the criteria of proximity sometimes gave no solution, for example, two adjacent sites with very different ρ_a curves between them (f. ex., sites ROJ and PER) impeded sometimes the convergence of the Levenberg-Marquard algorithm. Such a case can lead also to a false solution seen in a large χ^2 misfit.
Taking the above conditions into account, the multiple site decomposition scheme for the short (50−1000 s) and long (1000−8000 s[2]) period band has been applied to a selected group of sites. The site combinations were grouped as shown in table 5.1.

Coastal Cordillera	Longitudinal Valley	Precordillera	Western Cordillera	Altiplano
HDN−PEN−GLO−LAY	CDL−CTE−PDT−SOL	SAU−685−CHI	SILA−BAT−LIR	CHU−PAY−JUL
PEN−GER−GLO−LAY	PAM−MAT−VIC	QCH−ALO−CAM	LIB−VER	KHA−KHU−MAN
ROJ−GER−CCY−BLA	MAT−PIC−QUU	QGA−JAC−QUE	MIM−VIS	GRA−YAN
PER−ENG−FOR	VIC−ORI−GOR	TIQ−HUA−COC	EPU−PAJ−HIU−MOP	VAD−RAM−KKO
RUI−PAM	CHA−KOZ−QDP	QBA−CAR	TAR−LUX−PAM	CAL−MIK−VIL−CAS
		INC−ALC		

Table 5.1: Site combinations considered in the multiple site telluric and magnetic tensor decomposition. The same arrays were also considered in the channeling analysis of section 6.3.

Some sites where considered in more than one combination. The best solutions (i.e., smaller χ^2 misfit) thereof have been underlined in table 5.1. The short and long period strike angles of the W-E profile stations are plotted in fig.5.8. The result has been considerably stabilized in comparison to the single site solution (fig.5.6). At the short period band, the strike angles vary between 0 and -15° from the Coastal Cordillera to the western Precordillera (fig.5.8). The average strike angle is around -8°, which was the same tensor rotation angle considered in the Pica profile for the 2-D modeling (Echternacht [1998]), obtained after the hypothetical event analysis (Ritter [1996]) of the magnetic transfer function data.
At the long period band solution, the strike angles range between -15° and 15° in: the Pica profile, between CC and LV in the middle profile, and between the coast and Precordillera in Ancorp. Near 30-40° strike angles are found in the Precordillera of the middle profile, and the Western Cordillera and western Altiplano of Ancorp (fig.5.8).

Analogous to the telluric tensor decomposition (section 5.2.1) near 30-40° strike angles were found at some sites located in the Precordillera, Western Cordillera and Altiplano. The 2-D superposition model in these regions is not valid, given the high χ^2-misfit values of the test of the hypothesis obtained.
The following chapter (6) focuses on an explanation for the strong galvanic distortion identified mainly in the Coastal Cordillera and Precordillera, inferred from the maximal shear angles observed. For it a current channeling analysis is theoretically proposed (section 6.1) to detect and identify the cause of the distortion. A qualitative impression of the anomalous

[2]The multiple site decomposition for the long period band is now 1000-8000 s instead of 1000−6000 s (as in the telluric decomposition), because the first period range led in general to more stable strike angles.

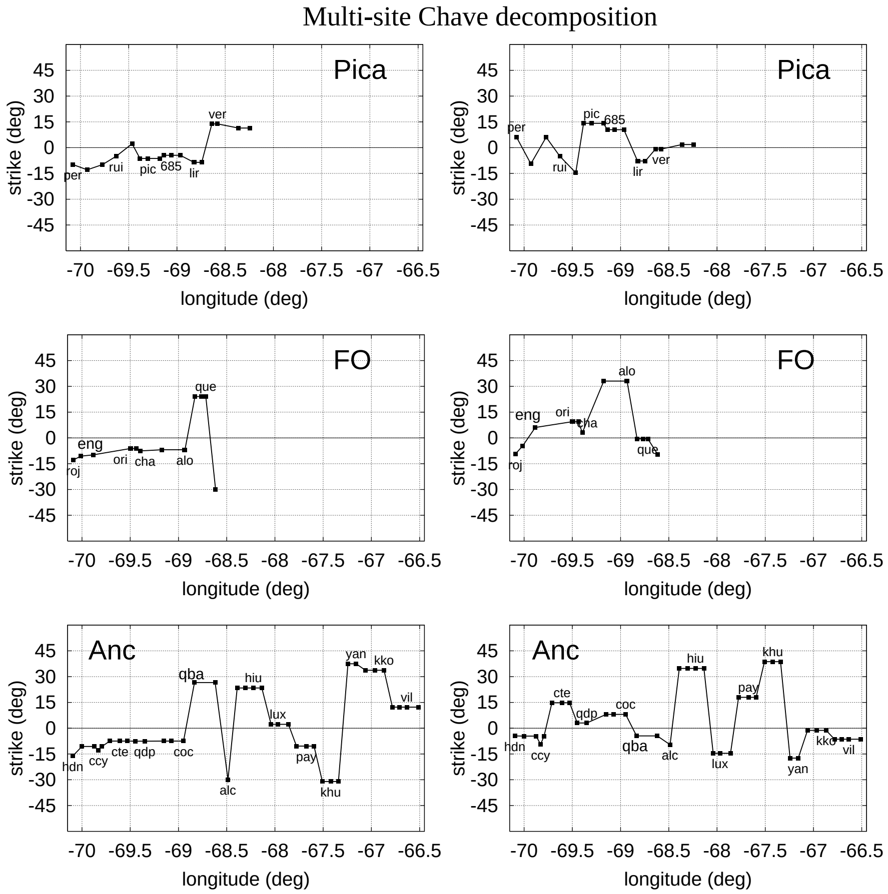

Figure 5.8: Multi-site telluric and magnetic tensor decomposition (Chave and Smith [1994]) of the Pica (above) and Ancorp (bottom) profile, and the W-E projection of the sites in between (center). *Left:* Procedure performed in the short period band (50−1000 s). *Right:* Procedure performed in the long period band (1000−8000 s).

conductivity structures in the region is extracted thereof (section 6.3).